

Exploiting Multiple Intelligent Reflecting Surfaces in Multi-Cell Uplink MIMO Communications

Junghoon Kim*, Seyyedali Hosseinalipour*, Taejoon Kim†, David J. Love* and Christopher G. Brinton*

*Electrical and Computer Engineering, Purdue University, West Lafayette, IN, USA

†Electrical Engineering and Computer Science, University of Kansas, Lawrence, KS, USA

*{kim3220, hosseina, djlove, cgb}@purdue.edu, †taejoonkim@ku.edu

Abstract—Applications of intelligent reflecting surfaces (IRSs) in wireless networks have attracted significant attention recently. Most of the relevant literature is focused on the single cell setting where a single IRS is deployed, while static and perfect channel state information (CSI) is assumed. In this work, we develop a novel methodology for *multi-IRS-assisted multi-cell networks* in the uplink. We formulate the sum-rate maximization problem aiming to jointly optimize the IRS reflect beamformers, base station (BS) combiners, and user equipment (UE) transmit powers. In this optimization, we consider the scenario in which (i) channels are dynamic and (ii) only partial CSI is available at each BS; specifically, scalar effective channels of local UEs and some of the interfering UEs. In casting this as a sequential decision making problem, we propose a multi-agent deep reinforcement learning algorithm to solve it, where each BS acts as an independent agent in charge of tuning the local UEs transmit powers, the local IRS reflect beamformer, and its combiners. We introduce an efficient message passing scheme that requires limited information exchange among the neighboring BSs to cope with the non-stationarity caused by the coupling of actions taken by multiple BSs. Our numerical simulations show that our method obtains substantial improvement in average data rate compared to several baseline approaches, e.g., fixed UEs transmit power and maximum ratio combining.

I. INTRODUCTION

Intelligent reflecting surfaces (IRSs) are one of the innovative technologies for 6G and beyond [1]–[4]. An IRS is an array of passive reflecting elements with a control unit. It can manipulate the propagation of an incident signal by providing an abrupt phase shift to change the propagation direction, which provides a function to control the communication channel. In current literature, IRSs are mostly utilized to provide enhanced communication efficiency without building extra, costly infrastructure [5]–[9]. In this paper, we study a scenario where multiple IRSs are deployed in a multi-cell cellular setting to provide higher data rate to the users.

A. Related Work

Exploiting IRSs in cellular networks initiated with applications of this technology in the downlink (DL). Studying IRS use cases in the uplink (UL) is thus comparably more recent.

1) *Utilizing IRSs in DL*: Most of the relevant literature has considered a *single cell* system with a *single IRS* [5], [6], [10]. Specific investigations have included quality of service (QoS)-constrained transmit power minimization [5], weighted sum-rate maximization [6], and symbol error rate minimization [10] to obtain the base station (BS) beamformer and IRS reflect

beamformer/precoder on the DL. Unlike the prior approaches, the work in [7] considers a *multi-cell* scenario with a single IRS, where the BS precoders and IRS reflect beamformer are designed to maximize (weighted) sum rate.

2) *Utilizing IRSs in UL*: Most of the works in UL design are also focused on single cell systems with a single IRS [11]–[15]. Several of these works have studied IRS reflect beamformer design and uplink user power control problems [11], [16], where the impact of quantized IRS phase values [12] and compressed sensing-based user detection [15] on the uplink data rate have also been investigated. The concept of IRS resembles analog beamforming in millimeter-wave (mmWave)-based systems [13], and this similarity has been explored in [11] to mitigate mmWave physical blockage. Recently, systems with two IRSs are considered, with the primary focus on efficient channel estimation of IRSs [17] and SINR fairness [18].

So far, there have not been any studies on multi-IRS deployment in multi-cell scenarios in UL. Despite the potential benefit of improving multi-cell-wide performance, this analysis has been beset with difficulty due to the added optimization complexity involved in controlling multiple IRSs.

B. Overview of Methodology and Contributions

We consider a novel architecture for multi-IRS-assisted multi-cell networks in UL. We further complement our framework via explicit consideration of multiple reflections among IRSs, which is rarely considered in existing literature. We formulate the sum-rate maximization problem aiming to jointly optimize user equipment (UE) transmit powers, IRS reflect beamformers, and BS combiners across cells. We consider the scenario where (i) channels are time-varying, and (ii) only partial/imperfect CSI is available, in which each BS only has the knowledge of scalar effective channels of local UEs and some of interfering UEs from neighboring cells. This is clearly more practical and realistic as compared to the prior approaches [12]–[16] that assume static and perfect knowledge of all channel matrices.

Given the interdependencies between the design variables across different cells, we cast the problem as sequential decision making and tailor a multi-agent deep reinforcement learning (DRL) algorithm to solve it. We consider each BS as an independent learning agent that controls the local UE transmit powers, the local IRS reflect beamformer, and its

combiners. We design the state, action, and reward function for each BS to capture the interdependencies among the design choices made at different BSs. We further develop a message-passing scheme where only limited information among neighboring BSs is exchanged to cope with the non-stationarity issue caused by the coupling between the actions at other BSs. Through numerical simulations, we show that our proposed scheme outperforms the conventional baselines for data rate maximization.

II. MULTI-CELL SYSTEMS WITH MULTIPLE IRSs

In this section, we first introduce the signal model under consideration (Sec. II-A). Then, we formulate the optimization and discuss the challenges associated with solving it (Sec. II-B).

A. Signal Model

We consider a multi-cell system with multiple IRSs for the uplink (UL) as depicted in Fig. 1. The system is comprised of a set of L cells $\mathcal{L} = \{1, \dots, L\}$ and R IRSs $\mathcal{R} = \{1, \dots, R\}$. For simplicity we assume that each cell has one IRS, i.e., $R = L$, though our method can be readily generalized to the case where $R \neq L$. It is assumed that the IRSs are indexed such that cell ℓ contains IRS ℓ . Each cell $\ell \in \mathcal{L}$ contains (i) K_ℓ UEs with single antenna, denoted by $\mathcal{K}_\ell = \{1, \dots, K_\ell\}$, (ii) an IRS with N_ℓ reflecting elements, denoted by $\mathcal{N}_\ell = \{1, \dots, N_\ell\}$, and (iii) a BS with M_ℓ antennas denoted by $\mathcal{M}_\ell = \{1, \dots, M_\ell\}$. We let UE (i, j) refer to UE j in cell i . The received signal vector at BS $\ell \in \mathcal{L}$ at the t th channel instance is given by

$$\begin{aligned} \mathbf{y}_\ell[t] = & \sum_{i \in \mathcal{L}} \sum_{j \in \mathcal{K}_\ell} \sqrt{p_{i,j}[t]} \mathbf{h}_{(i,j),\ell}^{\text{UB}}[t] s_{i,j}[t] \\ & + \sum_{r \in \mathcal{R}} \sum_{i \in \mathcal{L}} \sum_{j \in \mathcal{K}_i} \sqrt{p_{i,j}[t]} \mathbf{G}_{r,\ell}^{\text{IB}} \mathbf{\Phi}_r[t] \mathbf{h}_{(i,j),r}^{\text{UI}}[t] s_{i,j}[t] \\ & + \sum_{r_2 \in \mathcal{R}} \sum_{r_1 \in \mathcal{R} \setminus \{r_2\}} \sum_{i \in \mathcal{L}} \sum_{j \in \mathcal{K}_i} \sqrt{p_{i,j}[t]} \left(\mathbf{G}_{r_2,\ell}^{\text{IB}} \mathbf{\Phi}_{r_2}[t] \mathbf{G}_{r_1,r_2}^{\text{II}} \mathbf{\Phi}_{r_1}[t] \right. \\ & \left. \mathbf{h}_{(i,j),r_1}^{\text{UI}}[t] s_{i,j}[t] \right) + \mathbf{n}_\ell[t], \quad (1) \end{aligned}$$

where $\mathbf{h}_{(i,j),\ell}^{\text{UB}}[t] \in \mathbb{C}^{M_\ell \times 1}$ is the direct channel from UE (i, j) to BS ℓ , $\mathbf{h}_{(i,j),r}^{\text{UI}}[t] \in \mathbb{C}^{N_r \times 1}$ is the channel from UE (i, j) to IRS $r \in \mathcal{R}$, $\mathbf{G}_{r,\ell}^{\text{IB}} \in \mathbb{C}^{M_\ell \times N_r}$ is the channel from IRS r to BS ℓ , and $\mathbf{G}_{r_1,r_2}^{\text{II}} \in \mathbb{C}^{N_{r_2} \times N_{r_1}}$ is the channel from IRS r_1 to IRS r_2 , $r_1 \neq r_2$. Also, $p_{i,j}[t] \in \mathbb{R}^+$ is the transmit power and $s_{i,j}[t] \in \mathbb{C}$ is the transmit symbol of UE (i, j) , where $\mathbb{E}[|s_{i,j}[t]|^2] = 1$. The noise vector $\mathbf{n}_\ell[t] \in \mathbb{C}^{M_\ell \times 1}$ at BS ℓ is assumed to be distributed according to zero mean complex Gaussian with covariance matrix $\sigma^2 \mathbf{I}$, i.e., $\mathbf{n}_\ell[t] \sim \mathcal{CN}(\mathbf{0}, \sigma^2 \mathbf{I})$, where \mathbf{I} denotes the identity matrix and σ^2 is the noise variance. In (1), $\mathbf{\Phi}_r[t] = \text{diag}(\phi_{r,1}[t], \phi_{r,2}[t], \dots, \phi_{r,N_r}[t]) \in \mathbb{C}^{N_r \times N_r}$ is a diagonal matrix with its diagonal entries representing the beamforming vector of IRS $r \in \mathcal{R}$, where $\phi_{r,n}[t]$, $n \in \mathcal{N}_r$, is modeled as $\phi_{r,n}[t] = a_{r,n}[t] e^{j2\pi\theta_{r,n}[t]} \in \mathbb{C}$, incurring the signal attenuation $a_{r,n}[t] \in [0, 1]$ and phase shift $\theta_{r,n}[t] \in [0, 2\pi)$.

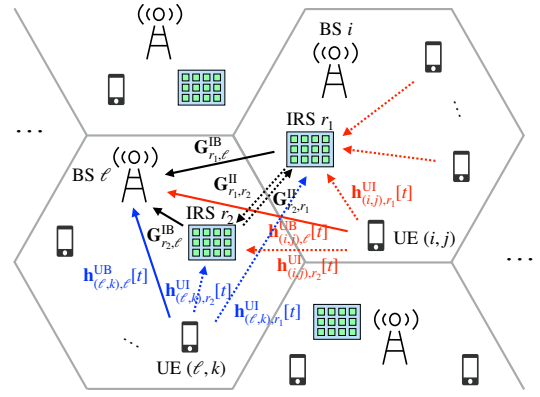


Fig. 1: A schematic of a multi-IRS-aided multi-cell system in UL.

The first nested sum in (1) captures the composite signal directly received from UEs and the second nested sum is the sum of signals from UEs directly received after one reflection from the IRSs. The third nested sum is the sum of received signals from UEs reflected twice by the IRSs. Higher order reflections can also be incorporated in (1), i.e., signals reflected from more than two IRSs. We consider up to the second order reflections due to a large path loss induced by multiple reflections between IRSs.

We assume that a linear combiner $\mathbf{z}_{\ell,k}[t] \in \mathbb{C}^{M_\ell \times 1}$ is employed at BS ℓ to restore $s_{\ell,k}[t]$ from $\mathbf{y}_\ell[t]$, which yields

$$\hat{y}_{\ell,k}[t] = \mathbf{z}_{\ell,k}^H[t] \mathbf{y}_\ell[t], \quad (2)$$

where superscript H denotes the conjugate transpose.

B. Problem Formulation and Challenges

We aim to maximize the sum-rate over all the UEs in the network by designing UE powers $\{p_{\ell,k}[t]\}_{\ell,k}$, BS combiners $\{\mathbf{z}_{\ell,k}[t]\}_{\ell,k}$, and IRS beamformers $\{\phi_r[t]\}_r$, where $\phi_r[t] = [\phi_{r,1}[t], \phi_{r,2}[t], \dots, \phi_{r,N_r}[t]]^\top \in \mathbb{C}^{N_r \times 1}$ is the IRS beamforming vector on the diagonal of $\mathbf{\Phi}_r[t]$, i.e., $\mathbf{\Phi}_r[t] = \text{diag}(\phi_r[t])$. With $\text{SINR}_{\ell,k}[t]$ as the signal-to-interference ratio (SINR) of UE (ℓ, k) , we propose the following optimization problem:

$$\begin{aligned} & \text{maximize} && \sum_{\ell \in \mathcal{L}} \sum_{k \in \mathcal{K}_\ell} \log_2(1 + \text{SINR}_{\ell,k}[t]) \quad (3) \\ & \text{subject to} && p_{\ell,k}[t] \in \mathcal{P}, \quad \forall \ell, k, \quad \mathbf{z}_{\ell,k}[t] \in \mathcal{Z}, \quad \forall \ell, k, \\ & && \phi_r[t] \in \mathcal{Q}, \quad \forall r, \\ & \text{variables} && \{p_{\ell,k}[t]\}_{\ell,k}, \{\mathbf{z}_{\ell,k}[t]\}_{\ell,k}, \{\phi_r[t]\}_r, \end{aligned}$$

where \mathcal{P} is the feasible set of power values, \mathcal{Z} is the codebook for BS combiners, and \mathcal{Q} is the codebook for IRS beamformers.

The problem in (3) is an optimization problem at time t , for $t \in \mathcal{T} = \{0, T, 2T, \dots\}$, where optimization of variables is performed once every T time instances. Given stationary channels $\mathbf{G}_{r,\ell}^{\text{IB}}$ and $\mathbf{G}_{r_1,r_2}^{\text{II}}$, if the instantaneous channels $\mathbf{h}_{(i,j),\ell}^{\text{UB}}[t]$, $\mathbf{h}_{(i,j),r}^{\text{UI}}[t]$ are known, the problem becomes one-shot optimization at each t . This is because $\text{SINR}_{\ell,k}[t]$ in the objective function can be formulated as (4) with the known

$$\text{SINR}_{\ell,k}[t] = \frac{p_{\ell,k}[t] \left| \mathbf{z}_{\ell,k}^H[t] \left(\mathbf{h}_{(\ell,k),\ell}^{\text{UB}}[t] + \sum_{r \in \mathcal{R}} \mathbf{G}_{r,\ell}^{\text{IB}} \Phi_r[t] \mathbf{h}_{(\ell,k),r}^{\text{UI}}[t] + \sum_{r_2 \in \mathcal{R}} \sum_{r_1 \in \mathcal{R} \setminus \{r_2\}} \mathbf{G}_{r_2,\ell}^{\text{IB}} \Phi_{r_2}[t] \mathbf{G}_{r_1,r_2}^{\text{II}} \Phi_{r_1}[t] \mathbf{h}_{(\ell,k),r_1}^{\text{UI}}[t] \right) \right|^2}{\sum_{(i,j) \neq (\ell,k)} p_{i,j}[t] \left| \mathbf{z}_{\ell,k}^H[t] \left(\mathbf{h}_{(i,j),\ell}^{\text{UB}}[t] + \sum_{r \in \mathcal{R}} \mathbf{G}_{r,\ell}^{\text{IB}} \Phi_r[t] \mathbf{h}_{(i,j),r}^{\text{UI}}[t] + \sum_{r_2 \in \mathcal{R}} \sum_{r_1 \in \mathcal{R} \setminus \{r_2\}} \mathbf{G}_{r_2,\ell}^{\text{IB}} \Phi_{r_2}[t] \mathbf{G}_{r_1,r_2}^{\text{II}} \Phi_{r_1}[t] \mathbf{h}_{(i,j),r_1}^{\text{UI}}[t] \right) \right|^2 + \sigma^2} \quad (4)$$

channels. In this case, conventional optimization methods, e.g., successive convex approximation and integer programming, could be applied. Nevertheless, implementing IRS-assisted wireless networks faces the following challenges in practice:

- *IRS channel acquisition*: Although most of the works, e.g., [12]–[16], assume that channels are perfectly known, this assumption is impractical because an IRS is passive and often does not have RF chains to sense signals. Even though special IRS hardware may be equipped with the ability to estimate the concatenated channels [19], the time overhead could easily overwhelm the coherent channel resources especially where there are multiple IRSs.
- *Dynamic channels*: Channel dynamics in wireless environments adds another degree of difficulty to channel acquisition and estimation. This makes solving the optimization in (3) impossible with conventional model-based optimization approaches, due to dynamic and unknown channels.
- *Centralization*: A centralized implementation to solve (3) would require gathering of all the information at a central point that is impractical in our setting. Given the interdependencies among the design variables taken by different cells and their impact on the overall objective function, joint design of the optimization variables in (3) is challenging.

To address these challenges, we convert (3) into a *sequential decision making problem*, where the variable design is carried out through successive interactions with the environment by utilizing a model-free learning method, i.e., *deep reinforcement learning* (DRL). While conventional DRL assumes a centralized implementation, we develop a *multi-agent DRL*, where each BS acts as an independent agent in charge of tuning its local UEs transmit powers, local IRS reflect beamformer, and combiners. Given the interdependencies between the actions taken by the BSs, we carry out the learning through limited message passing among the neighbouring BSs, which enables our method to cope with the *non-stationarity* issue of multi-agent DRL [20].

III. MULTI-AGENT DRL FRAMEWORK DESIGN

In this section, we first introduce the information collection process at the BSs and design a limited message passing scheme among the neighboring BSs, both of which are used to perform sequential decision making (Sec. III-A). We then formulate a Markov decision process (MDP) (Sec. III-B) and propose a dynamic control scheme based on multi-agent DRL (Sec. III-C).

A. Local Observations and Information Exchange

BS ℓ collects *scalar effective channels* as available information in real-time. Specifically, when UE (i, j) transmits a pilot

symbol with power $p_{i,j}[t]$, BS ℓ measures the scalar effective channel $\hat{h}_{(i,j),\ell,k}[t] \in \mathbb{C}$ (after combining) with combiner $\mathbf{z}_{\ell,k}[t]$, $k \in \mathcal{K}_\ell$, which is given by

$$\hat{h}_{(i,j),\ell,k}[t] = \mathbf{z}_{\ell,k}^H[t] \hat{\mathbf{h}}_{(i,j),\ell}[t], \quad (5)$$

where $\hat{\mathbf{h}}_{(i,j),\ell}[t] \in \mathbb{C}^{N_T \times 1}$ is the *effective channel* from UE (i, j) to BS ℓ (before combining), which is expressed as follows:

$$\hat{\mathbf{h}}_{(i,j),\ell}[t] = \sqrt{p_{i,j}[t]} \left(\mathbf{h}_{(i,j),\ell}^{\text{UB}}[t] + \sum_{r \in \mathcal{R}} \mathbf{G}_{r,\ell}^{\text{IB}} \Phi_r[t] \mathbf{h}_{(i,j),r}^{\text{UI}}[t] + \sum_{r_2 \in \mathcal{R}} \sum_{r_1 \in \mathcal{R} \setminus \{r_2\}} \mathbf{G}_{r_2,\ell}^{\text{IB}} \Phi_{r_2}[t] \mathbf{G}_{r_1,r_2}^{\text{II}} \Phi_{r_1}[t] \mathbf{h}_{(i,j),r_1}^{\text{UI}}[t] \right). \quad (6)$$

To carry out the information collection and exchange processes, we define two sets of cell indices. For information collection, we define the set of indices of *interfering* neighboring cells $\mathcal{B}_\ell^{(1)}[t]$ in which UEs are interfering with the data link from local UEs in cell ℓ to BS ℓ . Formally, $\forall i \in \mathcal{B}_\ell^{(1)}[t], \forall i' \in \mathcal{L} \setminus \mathcal{B}_\ell^{(1)}[t] \setminus \{\ell\} : \sum_{j \in \mathcal{K}_i} \|\hat{\mathbf{h}}_{(i,j),\ell}[t]\|_2^2 \geq \sum_{j \in \mathcal{K}_{i'}} \|\hat{\mathbf{h}}_{(i',j),\ell}[t]\|_2^2$. In other words, $\mathcal{B}_\ell^{(1)}[t]$ contains the indices of the cells with the dominant interfering effect on the links in cell ℓ . The size of this set is a control variable $B^{(1)} = |\mathcal{B}_\ell^{(1)}[t]|$. For information exchange, we define the set of indices of *interfered* neighboring cells $\mathcal{B}_\ell^{(2)}[t]$ that are interfered with by UEs in cell ℓ : $\forall i \in \mathcal{B}_\ell^{(2)}[t], \forall i' \in \mathcal{L} \setminus \mathcal{B}_\ell^{(2)}[t] \setminus \{\ell\} : \sum_{k \in \mathcal{K}_{i'}} \|\hat{\mathbf{h}}_{(\ell,k),i'}[t]\|_2^2 \geq \sum_{k \in \mathcal{K}_\ell} \|\hat{\mathbf{h}}_{(\ell,k),i'}[t]\|_2^2$. In other words, $\mathcal{B}_\ell^{(2)}[t]$ contains the indices of the cells in which the data links experience the most interference from the UEs in cell ℓ . The size of this set is a control variable $B^{(2)} = |\mathcal{B}_\ell^{(2)}[t]|$.

We consider that BS ℓ measures the scalar effective channels from (i) local UEs (ℓ, k) , $k \in \mathcal{K}_\ell$, and (ii) UEs (i, j) in neighboring cells, $i \in \mathcal{B}_\ell^{(1)}[t]$, $j \in \mathcal{K}_i$. The effective channel power, used in defining $\mathcal{B}_\ell^{(1)}[t]$ and $\mathcal{B}_\ell^{(2)}[t]$, can be acquired by the antenna circuit before digital processing, e.g., from the automatic gain control (AGC) circuit [21], without the explicit effective channel vector. BS ℓ also measures SINR $_{\ell,k}[t]$ of all local UEs, by measuring the received signal strength indicator (RSSI) and the reference signal received power (RSRP), which are the conventional measures to evaluate the signal quality in LTE standards [22]. Using the SINRs, BS ℓ then calculates the maximum achievable data rate of UE (ℓ, k) as $R_{\ell,k}[t] = \log_2(1 + \text{SINR}_{\ell,k}[t])$.¹

BS ℓ also receives limited information from neighboring BS $i \in \mathcal{B}_\ell^{(2)}[t]$: (i) *the scalar effective channel powers* from UEs

¹We omit the bandwidth parameter, assuming the same bandwidth for all the data links.

in cell ℓ to BS i , $\{\hat{h}_{(\ell,k),i,j}[t-T]\}_{k \in \mathcal{K}_\ell, j \in \mathcal{K}_i}$, and (ii) a penalty value, $P_{\ell,i}[t-T]$. $P_{\ell,i}[t-T]$ is used for designing the reward function and will be formalized in Sec. III-B3.

B. Markov Decision Process Model

We formulate the decision making process of each BS as an MDP with states, actions, and rewards:

1) *State*: We define the state space of BS ℓ as

$$\mathcal{S}_\ell[t] = \mathcal{S}_{\ell,1}[t] \cup \mathcal{S}_{\ell,2}[t] \cup \mathcal{S}_{\ell,3}[t] \cup \mathcal{S}_{\ell,4}[t], \quad (7)$$

$\mathcal{S}_\ell[t] = \mathcal{S}_{\ell,1}[t] \cup \mathcal{S}_{\ell,2}[t] \cup \mathcal{S}_{\ell,3}[t] \cup \mathcal{S}_{\ell,4}[t]$, where each constituent set of information is described below.

(i) **Local channel information.** $\mathcal{S}_{\ell,1}[t]$ consists of the scalar effective channel powers from local UEs observed at time $t-T$ and time t , given by $\mathcal{S}_{\ell,1}[t] = \{\hat{h}_{(\ell,j),\ell,k}[t-T]\}_{k,j \in \mathcal{K}_\ell} \cup \{\tilde{h}_{(\ell,j),\ell,k}[t]\}_{k,j \in \mathcal{K}_\ell}$. $\hat{h}_{(\ell,j),\ell,k}[t-T]$ can be obtained from (5). $\tilde{h}_{(\ell,j),\ell,k}[t]$ is a version of (5) obtained at time t using outdated variables $p_{\ell,k}[t-T]$, $\mathbf{z}_{\ell,k}[t-T]$, and $\{\phi_r[t-T]\}_{r \in \mathcal{R}}$ at the UE, BS, and IRSs. These two scalar effective channel powers contain different channel instances, i.e., $\mathbf{h}_{(i,j),\ell}^{\text{UB}}[t-T]$ and $\mathbf{h}_{(i,j),\ell}^{\text{UI}}[t-T]$ in $\hat{h}_{(\ell,j),\ell,k}[t-T]$, and $\mathbf{h}_{(i,j),\ell}^{\text{UB}}[t]$ and $\mathbf{h}_{(i,j),\ell}^{\text{UI}}[t]$ in $\tilde{h}_{(\ell,j),\ell,k}[t]$. Having them enables us to capture the effect of channel variation over time.

(ii) **From-neighbor channel information.** $\mathcal{S}_{\ell,2}[t]$ contains the scalar effective channel powers from UE (i,j) in neighboring cell i , and the index i , $i \in \mathcal{B}_\ell^{(1)}[t]$, $j \in \mathcal{K}_i$. Formally, $\mathcal{S}_{\ell,2}[t] = \{\hat{h}_{(i,j),\ell,k}[t-T]\}_{j \in \mathcal{K}_i, k \in \mathcal{K}_\ell, i \in \mathcal{B}_\ell^{(1)}[t]} \cup \{i\}_{i \in \mathcal{B}_\ell^{(1)}[t]}$. This set captures the interference of neighbor UEs on cell ℓ .

(iii) **To-neighbor channel information.** $\mathcal{S}_{\ell,3}[t]$ contains the scalar effective channel powers from local UE (ℓ,k) to BS i , and the index i , $i \in \mathcal{B}_\ell^{(2)}[t]$, $k \in \mathcal{K}_\ell$. Formally, $\mathcal{S}_{\ell,3}[t] = \{\hat{h}_{(\ell,k),i,j}[t-T]\}_{j \in \mathcal{K}_i, k \in \mathcal{K}_\ell, i \in \mathcal{B}_\ell^{(2)}[t]} \cup \{i\}_{i \in \mathcal{B}_\ell^{(2)}[t]}$. This set captures the amount of interference that local UEs in cell ℓ incur on neighboring cells. This information enables BS ℓ to adjust the transmit powers of local UEs to reduce interference on the neighboring cells.

(iv) **Previous local variables and local sum-rate.** $\mathcal{S}_{\ell,4}[t]$ consists of previous local variables, i.e., $\{p_{\ell,k}[t-T]\}_{k \in \mathcal{K}_\ell}$, $\{\mathbf{z}_{\ell,k}[t-T]\}_{k \in \mathcal{K}_\ell}$, and $\phi_\ell[t-T]$, and the local sum-rate $R_\ell[t-T] = \sum_{k \in \mathcal{K}_\ell} R_{\ell,k}[t-T]$. Formally, $\mathcal{S}_{\ell,4}[t] = \{p_{\ell,k}[t-T]\}_{k \in \mathcal{K}_\ell} \cup \{\mathbf{z}_{\ell,k}[t-T]\}_{k \in \mathcal{K}_\ell} \cup \{\phi_\ell[t-T]\} \cup \{R_\ell[t-T]\}$.

2) *Action*: The action space is defined as

$$\mathcal{A}_\ell[t] = \{b_{\ell,1}^p[t], \dots, b_{\ell,K_\ell}^p[t], b_{\ell,1}^z[t], \dots, b_{\ell,K_\ell}^z[t], b_\ell^\phi[t]\}, \quad (8)$$

where $b_{\ell,k}^p[t]$, $b_{\ell,k}^z[t]$, $b_\ell^\phi[t]$ are the *index control variables* used for updating the local UE (ℓ,k) transmit power, combiner k of BS ℓ , and local IRS ℓ reflect beamformer. These index control variables can take binary $\{-1, 1\}$, or ternary $\{-1, 0, 1\}$ alphabet as we will describe in Sec. IV.

Once BS ℓ determines the action in (8), the BS feeds forward $b_{\ell,k}^p[t]$ to UE (ℓ,k) , which then updates its power index as $i_{\ell,k}^p[t] = i_{\ell,k}^p[t-T] + b_{\ell,k}^p[t]$. The power of UE (ℓ,k) is set to $p_{\ell,k}[t] = \mathcal{P}(i_{\ell,k}^p[t])$, $k \in \mathcal{K}_\ell$, where $\mathcal{P}(i)$ denotes i -th element of the power set \mathcal{P} in (3). BS ℓ feeds forward $b_\ell^\phi[t]$ to IRS ℓ , which then updates its beamformer index as

$i_\ell^\phi[t] = i_\ell^\phi[t-T] + b_\ell^\phi[t]$. The beamformer of IRS ℓ is set to $\phi_\ell[t] = \mathcal{Q}(i_\ell^\phi[t])$, where $\mathcal{Q}(i)$ is the i -th vector in the codebook \mathcal{Q} in (3). Similarly, the combiner index is updated as $i_{\ell,k}^z[t] = i_{\ell,k}^z[t-T] + b_{\ell,k}^z[t]$. The combiner k of BS ℓ is set to $\mathbf{z}_{\ell,k}[t] = \mathcal{Z}(i_{\ell,k}^z[t])$.

3) *Reward*: BS ℓ aims to maximize the sum-rate in its own cell by controlling BS combiners, UE powers, and IRS beamformers. However, this could increase the interference to the neighboring cells. Thus, we design the reward $r_\ell[t]$ by including the penalty terms as follows:

$$r_\ell[t] = \sum_{k \in \mathcal{K}_\ell} R_{\ell,k}[t] - \sum_{i \in \mathcal{B}_\ell^{(2)}[t]} P_{\ell,i}[t], \quad (9)$$

where the first term is the sum-rate of cell ℓ and the second term is the sum of penalties. The penalty $P_{\ell,i}[t]$ is the rate loss in cell i caused by local UEs in cell ℓ calculated at BS i as

$$P_{\ell,i}[t] = \sum_{j \in \mathcal{K}_i} P_{\ell,(i,j)}[t] = \sum_{j \in \mathcal{K}_i} \left[-R_{i,j}[t] + \log_2 \left(1 + \frac{|\hat{h}_{(i,j),i,j}[t]|^2}{\sum_{(i',j') \neq (i,j), i' \neq \ell} |\hat{h}_{(i',j'),i,j}[t]|^2 + \sigma^2} \right) \right], \quad (10)$$

where $P_{\ell,(i,j)}[t]$ is the rate loss caused by all the UEs in cell ℓ on the data rate of UE (i,j) . The $\log(\cdot)$ term in (10) denotes the data rate of UE (i,j) without the interferences from the UEs in cell ℓ , while $R_{i,j}[t]$ is the data rate including the interferences from the UEs in cell ℓ . Without the interference from cell ℓ , the two terms cancel with each other, leading to a zero penalty term. Otherwise, the penalty is positive.

C. Dynamic Control Scheme based on Multi-agent DRL

In the proposed MDP, the channel values used as states are continuous variables making conventional RL that utilizes Q-learning with Q-table irrelevant. We thus adopt deep Q-network (DQN) [23]. BS ℓ possesses its own train DQN, $Q(s, a, \mathbf{w}_\ell)$ with weights \mathbf{w}_ℓ and target DQN, $Q(s, a, \mathbf{w}_\ell^-)$ with weights \mathbf{w}_ℓ^- , where the state $s \in \mathcal{S}$ and action $a \in \mathcal{A}$ are defined above. The pseudocode of the proposed dynamic control scheme based on multi-agent DRL is provided in Algorithm 1.

IV. NUMERICAL EVALUATION AND DISCUSSION

In this section, we first describe the simulation setup (Sec. IV-A) and evaluation scenarios (Sec. IV-B). Then, we present and discuss the results (Sec. IV-C).

A. Simulation Setup

1) *Parameter settings*: We consider a cellular network with $L = 7$ hexagonal cells, as shown in Fig. 2(a). We assume $K_\ell = 3$, $M_\ell = 5$, and $N_r = 5$, $\forall \ell, r$. The BSs are located at the center of each cell with 10 m height, and the distance between adjacent BSs is 100 m. Each IRS is deployed nearby the BS. The UEs are randomly placed in the cells. The set \mathcal{P} for power control is given by $\mathcal{P} = \{p_{\min}, p_{\min} e^{\Delta_p}, p_{\min} e^{2\Delta_p}, \dots, p_{\max}\}$, where $p_{\min} = 10$ dBm and $p_{\max} = 30$ dBm are the minimum

Algorithm 1 Dynamic control based on multi-agent DRL.

- 1: Establish a train DQN with weights \mathbf{w}_ℓ , a target DQN with weights \mathbf{w}_ℓ^- , an empty experience pool \mathcal{Y}_ℓ with $|\mathcal{Y}_\ell| = 0$, and a pool size M_ℓ^{pool} . Initialize the train DQN and target DQN with random weights. Set the discount factor γ_ℓ , initial ϵ -greedy value $\epsilon_\ell(0)$, mini-batch size M_ℓ^{batch} , and DQN-aligning period T_{align} , $\forall \ell \in \mathcal{L}$.
- 2: Agent ℓ (BS ℓ) randomly initializes the design variables $\{\mathbf{p}_{\ell,k}[0]\}_{k \in \mathcal{K}_\ell}$, $\{\mathbf{z}_{\ell,k}[0]\}_{k \in \mathcal{K}_\ell}$, and $\phi_\ell[0]$, and informs local UEs and local IRS of the initial variables, $\forall \ell \in \mathcal{L}$.
- 3: Agent ℓ selects its action $a_\ell \in \mathcal{A}$ randomly and executes it, $\forall \ell \in \mathcal{L}$.
- 4: $t \leftarrow T$. Agent ℓ observes the next state s'_ℓ , $\forall \ell \in \mathcal{L}$.
- 5: **repeat**
- 6: $s_\ell \leftarrow s'_\ell$
- 7: Agent ℓ selects its action a_ℓ at time t based on ϵ -greedy policy, $\forall \ell \in \mathcal{L}$: With probability $\epsilon_\ell(t)$, agent ℓ selects random action a_ℓ , and with probability $1 - \epsilon_\ell(t)$, agent ℓ selects $a_\ell = \arg \max_{a \in \mathcal{A}} Q(s_\ell, a, \mathbf{w}_\ell)$.
- 8: Agent ℓ executes its action, $\forall \ell \in \mathcal{L}$.
- 9: $t \leftarrow t + T$. Agent ℓ observes the next state s'_ℓ and gets the reward r_ℓ , $\forall \ell \in \mathcal{L}$.
- 10: Agent ℓ stores the new experience $\langle s_\ell, a_\ell, r_\ell, s'_\ell \rangle$ in its own experience pool \mathcal{Y}_ℓ , $\forall \ell \in \mathcal{L}$.
- 11: **if** $|\mathcal{Y}_\ell| \geq M_\ell^{\text{batch}}$ **then**
- 12: Agent ℓ samples a mini-batch consisting of M_ℓ^{batch} experiences from its experience pool \mathcal{Y}_ℓ , $\forall \ell \in \mathcal{L}$.
- 13: Agent ℓ updates the weights \mathbf{w}_ℓ of its train DQN using back propagation, $\forall \ell \in \mathcal{L}$.
- 14: Agent ℓ updates the weights of its target DQN $\mathbf{w}_\ell^- \leftarrow \mathbf{w}_\ell$ every T_{align} , $\forall \ell \in \mathcal{L}$.
- 15: **end if**
- 16: **until** system is terminated.

and maximum transmit power values of UEs, and $\Delta_p = (\log p_{\max} - \log p_{\min}) / (|\mathcal{P}| - 1)$. For BS combiner and IRS beamformer codebooks, we use a random vector quantization (RVQ) [24] codebook with size $|\mathcal{Z}| = |\mathcal{Q}| = 30$. The noise variance is $\sigma^2 = -114$ dBm. We consider $B^{(1)} = B^{(2)} = 2$.

2) *Channel modeling*: We consider a single frequency band with flat fading and adopt a temporally correlated block fading channel model. Following a cellular standard [25], we assume coherence time $T = 5$ ms and center frequency $f_c = 2.5$ GHz. The channel vector $\mathbf{h}_{(i,j),\ell}^{\text{BS}}[t]$ is modelled as follows:

$$\mathbf{h}_{(i,j),\ell}^{\text{UB}}[t] = \sqrt{\beta_{(i,j),\ell}^{\text{UB}}} \mathbf{u}_{(i,j),\ell}^{\text{UB}}[t], \quad (11)$$

where $\beta_{(i,j),\ell}^{\text{UB}}$ denotes the large-scale fading coefficient from UE (i, j) to BS ℓ , modeled as $\beta_{(i,j),\ell}^{\text{UB}} = \beta_0 - 10\alpha_{(i,j),\ell}^{\text{UB}} \log_{10}(d_{(i,j),\ell}^{\text{UB}}/d_0)$, where β_0 is the path-loss at the reference distance d_0 , $d_{(i,j),\ell}^{\text{UB}}$ is the distance between UE (i, j) and BS ℓ , and $\alpha_{(i,j),\ell}^{\text{UB}}$ is the path-loss exponent between them. We set $\beta_0 = -30$ dB and $d_0 = 1$ m. $\mathbf{u}_{(i,j),\ell}^{\text{UB}}[t]$ denotes the Rayleigh fading vector, and its evolution is modeled by a first-order Gauss-Markov process [26]:

$$\mathbf{u}_{(i,j),\ell}^{\text{UB}}[t] = \rho_{(i,j),\ell}^{\text{UB}} \mathbf{u}_{(i,j),\ell}^{\text{UB}}[t-T] + \sqrt{1 - (\rho_{(i,j),\ell}^{\text{UB}})^2} \mathbf{n}_{(i,j),\ell}^{\text{UB}}[t], \quad (12)$$

where $\mathbf{n}_{(i,j),\ell}^{\text{UB}}[t] \in \mathbb{C}^{M_\ell \times 1}$, $\mathbf{n}_{(i,j),\ell}^{\text{UB}}[t] \sim \mathcal{CN}(\mathbf{0}, \mathbf{I})$, and $\mathbf{u}_{(i,j),\ell}^{\text{UB}}[0] \sim \mathcal{CN}(\mathbf{0}, \mathbf{I})$. The time correlation coefficient $\rho_{(i,j),\ell}^{\text{UB}}$

obeys the Jakes model [26].² The same modeling for $\mathbf{h}_{(i,j),\ell}^{\text{UB}}[t]$ is applied for the channels between the UEs and the IRSs, i.e., $\mathbf{h}_{(i,j),r}^{\text{UI}}[t]$, $\forall i, j, r$, with path-loss exponent $\alpha_{(i,j),r}^{\text{UI}}$. $\mathbf{G}_{r_1,r_2}^{\text{IB}}$ and $\mathbf{G}_{r_1,r_2}^{\text{II}}$ are assumed to be stationary Rayleigh channels with each entry distributed according to $\mathcal{CN}(0, \beta_{r,\ell}^{\text{IB}})$ and $\mathcal{CN}(0, \beta_{r_1,r_2}^{\text{II}})$, respectively. $\beta_{r,\ell}^{\text{IB}}$ and $\beta_{r_1,r_2}^{\text{II}}$ denote the large-scale fading coefficients with path loss exponents $\alpha_{r,\ell}^{\text{IB}}$ and $\alpha_{r_1,r_2}^{\text{II}}$, respectively.

We assume $\alpha_{(i,j),\ell}^{\text{UB}} = \alpha^{\text{UB}}$, $\forall i, j, \ell$, $\alpha_{(i,j),r}^{\text{UI}} = \alpha^{\text{UI}}$, $\forall i, j, r$, $\alpha_{r,\ell}^{\text{IB}} = \alpha^{\text{IB}}$, $\forall r, \ell$, and $\alpha_{r_1,r_2}^{\text{II}} = \alpha^{\text{II}}$, $\forall r_1, r_2$. To model the presence of extensive obstacles and scatterers, the path-loss exponent between the UEs and BS is taken to be $\alpha^{\text{UB}} = 3.75$. Because the IRS-aided link can have less path loss than that of direct UE-BS channel by properly choosing the location of the IRS, we set the path-loss exponents of the UE-IRS link, of the IRS-BS link, and of the IRS-IRS link to $\alpha^{\text{UI}} = 2.2$, $\alpha^{\text{IB}} = 1$, and $\alpha^{\text{II}} = 2$, respectively [7]. We assume $\rho_{(i,j),\ell}^{\text{UB}} = \rho_{(i,j),r}^{\text{UI}} = \rho$, $\forall i, j, \ell, r$ and adopt $\rho = 0.999$ ($v \approx 1$ km/h), 0.99 ($v \approx 3$ km/h), and 0.9 ($v \approx 9$ km/h), where v is the UE speed.

B. Evaluation Scenarios

1) *Scenario 1. The effective channels from local UEs are not known*: In this scenario, each BS measures the scalar effective channels directly from received signals without explicitly obtaining the effective channels as a vector form in (6). We introduce two baselines in this scenario: RRR=(random, random, random) and MRR=(maximum, random, random). The name of each baseline is indicating how it selects its (UE power, IRS beamformer, and BS combiner) variables as a tuple. We propose DQN1, where the action space consists of $2K + 1$ elements for K UE powers, IRS beamformer, and K BS combiners. The index control variables are binary $\{-1, 1\}$.

2) *Scenario 2. The effective channels from local UEs are known*: In this scenario, each BS measures the effective channels from local UEs as the vector form in (6). Each BS is assumed to adopt a maximum ratio combiner (MRC) by finding the index $i^* = \arg \max_i |\mathcal{Z}(i)^H \mathbf{h}[t]|^2$ where $\mathbf{h}[t]$ is the effective channel from local UE. We introduce several baselines: MRM=(maximum, random, MRC), FRM=(1/4 maximum, random, MRC), RRM=(random, random, MRC), and MM with no IRS=(maximum, N/A, MRC). The MM with no IRS assumes the IRSs to be turned off. We propose DQN2 and DQN3. In DQN2, the action space consists of $K + 1$ elements for K UE powers and the IRS beamformer (the action space does not have the elements $b_{\ell,k}^z[t]$, $\forall k$ in (8)). The BS combiner is designed as MRC and the index control variable is binary $\{-1, 1\}$. The action space is DQN3 is the same as DQN2, except it uses a ternary index control variable $\{-1, 0, 1\}$.

In both scenarios, the DQNs³ are composed of an input

² $\rho_{(i,j),\ell}^{\text{UB}} = J_0(2\pi \tilde{f}_{(i,j)}^{\text{UB}} T)$, where $J_0(\cdot)$ is the zeroth order Bessel function of the first kind, and $\tilde{f}_{(i,j),\ell}^{\text{UB}} = v_{(i,j),\ell}^{\text{UB}} f_c / c$ is the maximum Doppler frequency, with velocity $v_{(i,j),\ell}^{\text{UB}}$ of UE (i, j) and $c = 3 \times 10^8$ m/s.

³All DQNs establish the same state space and reward function given in Sec. III-B. For the state information group (iv) in Sec. III-B1, the indices of previous local variables are stored in the state.

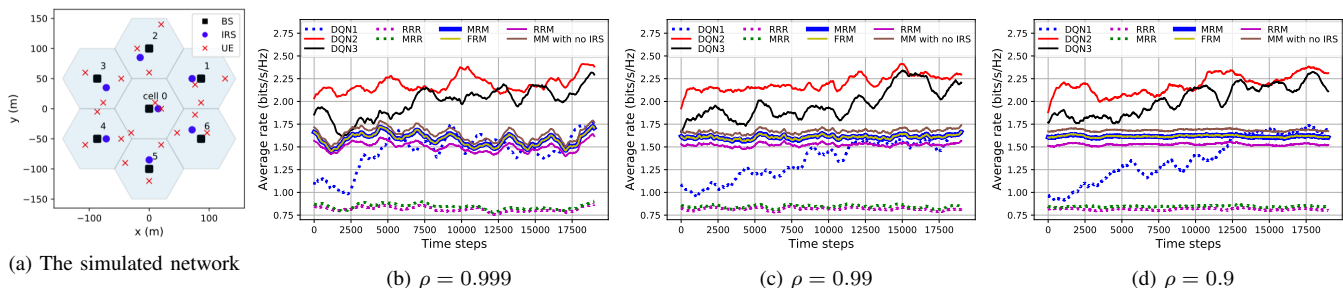


Fig. 2: (a): Cellular network with $L = 7$ hexagonal cells and 100 m distance between adjacent BSs used in our simulations. (b),(c),(d): Average achievable data rates over all 21 UEs obtained by each method. The dotted-lines and solid lines show the performance of schemes in Scenario 1 and Scenario 2, respectively. Each data point in the plots is a moving average over the previous 1000 time slots.

layer, an output layer, and two fully-connected hidden layers. The input size is $6K^2 + 2K + 6 = 66$. The output size is $2^{2K+1} = 128$, $2^{K+1} = 16$, and $3^{K+1} = 81$ for DQN1, DQN2, and DQN3, respectively. For DQN1, the number of neurons in the two hidden layers is 70 and 100; for DQN2, 40 and 30; and for DQN3, 70 and 70. The rectified linear unit (ReLU) activation function is employed. In Algorithm 1, we adopt the ϵ -greedy method with $\epsilon_\ell(t) = \max\{\epsilon_{\min}, (1 - 10^{-3.5})\epsilon_\ell(t-T)\}$, where $\epsilon_\ell(0) = 0.6$ and $\epsilon_{\min} = 0.005, \forall \ell$. The size of mini-batch is $M_\ell^{\text{batch}} = 10$, the experience pool size is $M_\ell^{\text{pool}} = 300$, and the discount factor is $\gamma_\ell = 0.7, \forall \ell$. We set $T_{\text{align}} = 50T$, i.e., the target DQN is updated with the weights of train DQN after $50T$. We employ the RMSProp optimizer.

C. Simulation Results and Discussion

Fig. 2(b),(c),(d) depict the average achievable data rate over all 21 UEs with different values of ρ . The dotted lines show the performance of the schemes in Scenario 1. With varying channels, RRR and MRR select random or fixed indices for variables, and therefore have low average data rates over time. On the other hand, DQN1 learns and adapts to the varying channels over time by exploiting the local observations and message passing in our sequential decision making.

The solid lines represent the performances of schemes in Scenario 2. The MM with no IRS gives better performance than the baselines using IRS, implying that random IRS beamforming is worse than not deploying it. This also reveals the vulnerability of IRS-assisted systems to adversarial IRS utilization. Our DQN2 and DQN3 methods outperform the baselines. DQN2 yields slightly better performance and converges faster than DQN3. The faster convergence is due to neural networks training faster with a smaller number of outputs. This better performance is also consistent with the observation [23] that DQNs are more successful with smaller action spaces.

Comparing Scenario 1 with 2, i.e., the dotted lines with the solid lines in Fig. 2(b),(c),(d), we note that the performance of DQN1, which only uses scalar effective channel powers, is comparable with the baselines in Scenario 2, which use vectorized local effective channels for MRC. Also, with higher ρ values, the DQNs experience faster convergence, which is

particularly noticeable in DQN1. The fluctuation of the DQN plots occurs due to the ϵ -greedy policy, which explores random action selection occasionally to avoid getting trapped in local optima. Overall, in each case, we see that our MDP-based algorithms obtain significant performance improvements, emphasizing the benefit of our multi-agent DRL method.

V. CONCLUSION

We developed a novel methodology for uplink multi-IRS-assisted multi-cell systems. Due to temporal channel variations and difficulties of channel acquisition, we proposed a dynamic control scheme based on multi-agent DRL, in which the actions are taken at BSs with limited message passing among them. In particular, each BS adaptively designs its local UE powers, local IRS beamformer, and its combiners. Through numerical simulations, we verified that our algorithm outperforms conventional baselines by adaptively controlling the variables.

ACKNOWLEDGMENT

D.J. Love was supported in part by the National Science Foundation (NSF) under grants CNS1642982 and CCF1816013.

REFERENCES

- [1] W. Saad, M. Bennis, and M. Chen, "A vision of 6G wireless systems: Applications, trends, technologies, and open research problems," *IEEE Network*, vol. 34, no. 3, pp. 134–142, 2020.
- [2] E. Basar, M. Di Renzo, J. De Rosny, M. Debbah, M. Alouini, and R. Zhang, "Wireless communications through reconfigurable intelligent surfaces," *IEEE Access*, vol. 7, pp. 116 753–116 773, 2019.
- [3] S. Hossainipour, C. G. Brinton, V. Aggarwal, H. Dai, and M. Chiang, "From federated to fog learning: Distributed machine learning over heterogeneous wireless networks," *IEEE Commun. Mag.*, 2020.
- [4] J. Zhang, E. Björnson, M. Matthaiou, D. W. K. Ng, H. Yang, and D. J. Love, "Prospective multiple antenna technologies for beyond 5G," *IEEE J. Sel. Areas Commun.*, vol. 38, no. 8, pp. 1637–1660, 2020.
- [5] Q. Wu and R. Zhang, "Intelligent reflecting surface enhanced wireless network via joint active and passive beamforming," *IEEE Trans. Wireless Commun.*, vol. 18, no. 11, pp. 5394–5409, 2019.
- [6] H. Guo, Y. Liang, J. Chen, and E. G. Larsson, "Weighted sum-rate maximization for intelligent reflecting surface enhanced wireless networks," in *Proc. IEEE Glob. Commun. Conf.*, 2019, pp. 1–6.
- [7] C. Pan, H. Ren, K. Wang, W. Xu, M. Elkashlan, A. Nallanathan, and L. Hanzo, "Multicell MIMO communications relying on intelligent reflecting surfaces," *IEEE Trans. Wireless Commun.*, 2020.

- [8] M. Cui, G. Zhang, and R. Zhang, "Secure wireless communication via intelligent reflecting surface," *IEEE Wireless Commun. Lett.*, vol. 8, no. 5, pp. 1410–1414, 2019.
- [9] X. Yu, D. Xu, Y. Sun, D. W. K. Ng, and R. Schober, "Robust and secure wireless communications via intelligent reflecting surfaces," *IEEE J. Sel. Areas Commun. (JSAC)*, 2020.
- [10] J. Ye, S. Guo, and M. S. Alouini, "Joint reflecting and precoding designs for SER minimization in reconfigurable intelligent surfaces assisted MIMO systems," *IEEE Trans. Wireless Commun.*, vol. 19, no. 8, pp. 5561–5574, 2020.
- [11] J. Xiong, L. You, Y. Huang, D. W. K. Ng, W. Wang, and X. Gao, "Reconfigurable intelligent surfaces assisted MIMO-MAC with partial CSI," in *Proc. IEEE Int. Conf. Commun. (ICC)*, 2020, pp. 1–6.
- [12] H. Zhang, B. Di, L. Song, and Z. Han, "Reconfigurable intelligent surfaces assisted communications with limited phase shifts: How many phase shifts are enough?" *IEEE Trans. Veh. Technol.*, vol. 69, no. 4, pp. 4498–4502.
- [13] K. Zhi, C. Pan, H. Ren, and K. Wang, "Uplink achievable rate of intelligent reflecting surface-aided millimeter-wave communications with low-resolution ADC and phase noise," *arXiv:2008.00437*, 2020.
- [14] Y. Cao and T. Lv, "Delay-constrained joint power control, user detection and passive beamforming in intelligent reflecting surface assisted uplink mmWave system," *arXiv:1912.10030*, 2019.
- [15] L. Feng, X. Que, P. Yu, W. Li, and X. Qiu, "IRS assisted multiple user detection for uplink URLLC non-orthogonal multiple access," in *IEEE Conf. Comput. Commun. Workshop*, 2020, pp. 1314–1315.
- [16] Y. Liu, J. Zhao, M. Li, and Q. Wu, "Intelligent reflecting surface aided MISO uplink communication network: Feasibility and SINR optimization," *arXiv:2007.01482*, 2020.
- [17] C. You, B. Zheng, and R. Zhang, "Wireless communication via double IRS: Channel estimation and passive beamforming designs," *arXiv:2008.11439*, 2020.
- [18] S. Zhang and R. Zhang, "Intelligent reflecting surface aided multi-user communication: Capacity region and deployment strategy," *arXiv:2009.02324*, 2020.
- [19] Z. Wang, L. Liu, and S. Cui, "Channel estimation for intelligent reflecting surface assisted multiuser communications: Framework, algorithms, and analysis," *IEEE Trans. Wireless Commun.*, 2020.
- [20] A. Marinescu, I. Dusparic, and S. Clarke, "Prediction-based multi-agent reinforcement learning in inherently non-stationary environments," *ACM Trans. Auton. Adapt. Syst.*, vol. 12, no. 2, pp. 1–23, 2017.
- [21] J. Mo, P. Schniter, and R. W. Heath, "Channel estimation in broadband millimeter wave MIMO systems with few-bit ADCs," *IEEE Trans. Signal Process.*, vol. 66, no. 5, pp. 1141–1154, 2017.
- [22] 3GPP TS 36.211, "LTE: Evolved universal terrestrial radio access (e-utra): Physical channels and modulation," vol. V14.2.0 Release 14, 2017.
- [23] V. Mnih, K. Kavukcuoglu, D. Silver, A. A. Rusu, J. Veness, M. G. Bellemare, A. Graves, M. Riedmiller, A. K. Fidjeland, G. Ostrovski *et al.*, "Human-level control through deep reinforcement learning," *nature*, vol. 518, no. 7540, pp. 529–533, 2015.
- [24] C. K. Au-Yeung and D. J. Love, "On the performance of random vector quantization limited feedback beamforming in a MISO system," *IEEE Trans. Wireless Commun.*, vol. 6, no. 2, pp. 458–462, 2007.
- [25] "IEEE P802.16m-2008 draft standard for local and metropolitan area network," *IEEE Standard 802.16m*, 2008.
- [26] B. Sklar *et al.*, *Digital communications: fundamentals and applications*, 2001.